

Nuclear Magnetic Resonance and Small-Angle Neutron Scattering Studies of Anionic Surfactants with Macrocounterions: Tetramethylammonium Dodecyl Sulfate

A. Paul* and P. C. Griffiths

School of Chemistry, Cardiff University, Main Building, Park Place, Cardiff, CF10 3AT, United Kingdom

E. Pettersson and P. Stilbs

Department of Physical Chemistry, Royal Institute of Technology (KTH), Stockholm, Sweden, S-100 44

Barney L. Bales

Center for Supramolecular Studies, Department of Physics & Astronomy, Northridge, California 91330-8268

R. Zana

Institut Charles Chadron, CNRS, Strasbourg, France

R. K. Heenan

Rutherford Appleton Laboratory, ISIS Facility, Chilton, Didcot, Oxford, OX1 0QX

Received: February 3, 2005; In Final Form: June 24, 2005

Micellar solutions of tetramethylammonium dodecyl sulfate have been studied to determine the degree of counterion binding. Tetramethylammonium chloride was added over a wide range of surfactant concentrations such that the total concentration of tetramethylammonium ions in solution remained constant. Small angle neutron scattering experiments showed a constancy in aggregation number across this series, consistent with the constant C_{aq} concept of Bales et al. (*J. Phys. Chem. B* **2001**, *105*, 6798). Pulsed-field gradient and electrophoretic NMR experiments were used to determine the degree of counterion dissociation, α , which was found to be 0.33. This value is in contrast to the value from conductivity measurements ($\alpha = 0.2$), but supports the concept of an aggregation number based definition of α .

Introduction

The properties and behavior of colloidal systems are dependent on their fundamental charge characteristics (swelling of polymeric microgels, suspension stability, surfactant solubility, micelle formation, and microemulsion phase behavior). Measuring these characteristics is not necessarily straightforward, especially for multicomponent systems where generally it is bulk charge properties that are measured. For example, classical methods for measuring counterion binding to micelles (e.g., conductivity) cannot accurately be applied to mixed surfactant systems as the micelle composition changes with dilution and the conductivity is dominated by the counterions, which are much more mobile than the micelles. Similarly, for polybases, pH titration inherently causes a simultaneous change in the ionic strength.

It is accepted that the charge of an ionic micelle arises from the distribution of counterions according to electrostatic interactions between headgroups and counterions at the micelle surface. The degree of counterion dissociation (α) is a fundamental property of an ionic surfactant, with important consequences for micelle formation and micellar growth. Variations between what are recognized by a given technique as “bound” and “dissociated” counterions often cause large discrepancies in absolute value of α measured by different techniques, although

it is accepted that, for most systems, α changes little with surfactant concentration, in line with theoretical arguments based on the Poisson–Boltzmann equation.

It was recently suggested that the degree of ionization or counterion dissociation of a surfactant micelle could be defined based on the aggregation number, N , using the hypothesis that N depends solely on the concentration of counterions in solution, C_{aq} , according to eq 1.¹

$$N = N(C_{\text{aq}}) \quad (1)$$

C_{aq} is calculated according to eq 2, taking into account contributions from monomeric surfactant, added salt, and any counterions dissociated from the micelles, and correcting the counterion concentration for the excluded volume of the micelles

$$C_{\text{aq}} = F(\alpha([\text{surfactant}] - [\text{monomer}]) + [\text{monomer}] + C_{\text{ad}}) \quad (2)$$

where $F = 1/(1 - \phi)$ is the correction factor for the micelle volume and C_{ad} the concentration of added salt.

It is hence possible to prepare a series of surfactant/salt solutions such that the overall free counterion concentration is invariant across a wide range of surfactant concentration.² According to eq 1 N remains invariant across this series and accordingly the micelle morphology should not change either. Further, it was recognized that for dodecyl sulfate micelles N

* Corresponding author. E-mail: paula3@cardiff.ac.uk.

varies according to the following power law²

$$N = N^0(C_{\text{aq}}/\text{cmc}_0)^\gamma \quad (3)$$

where N^0 denotes values at the cmc and γ is a constant. A recent study of sodium dodecyl sulfate (SDS), dodecyl trimethylammonium chloride (DTAC), and bromide (DTAB) used small-angle neutron scattering (SANS) coupled with time-resolved fluorescence quenching (TRFQ) to study SDS/NaCl, CTAB/NaBr, and CTAC/NaCl series.³ This paper demonstrated that these three surfactants behave as described by eq 3.

In a recent series of papers, Bales et. al have presented work on the solution properties of a series of tetraalkylammonium dodecyl sulfates (TAADS), surfactants with tetra methyl- (TMADS), ethyl- (TEADS), propyl- (TPADS), and butyl- (TBADS) ammonium counterions.^{4–7} For all of the TAADS there was a discrepancy between the value of α obtained at the cmc from conductivity measurements and those at higher surfactant concentrations (with and without added salt) obtained from EPR.⁵ For example, for TMADS, $\alpha_0 = 0.20$ from conductivity and $\alpha = 0.34$ from EPR. This discrepancy is the motivation for the present work. In the earlier work⁵ it was not possible to distinguish between two possibilities: (1) both conductivity and the aggregation number based determinations of α were correct, implying that α increases with aggregation number, or (2) either conductivity or aggregation number based determinations of α were incorrect. This latter possibility would cast doubt on the hypothesis that $N = N(C_{\text{aq}})$.

In this work we have chosen to study TMADS as a constant C_{aq} series with added tetramethylammonium chloride (TMACl). Small-angle neutron scattering (SANS) was performed to test the hypothesis that the TMADS micelles do not change either size or shape across the constant C_{aq} series. In addition PGSE-NMR and eNMR experiments were performed to provide independent values for α . As both the surfactant and counterion have NMR signals it is possible to obtain information on the charge and mobility of each species separately. The NMR techniques are therefore particularly sensitive to changes in α .

Materials

Tetramethylammonium dodecyl sulfate (TMADS) was synthesized and purified as described previously.⁴ Tetramethylammonium chloride (TMACl) was purchased from Aldrich and used as received. Samples were prepared in D₂O by diluting a stock surfactant solution with the appropriate salt solution. Since within a C_{aq} series $C_{\text{aq}} \equiv [\text{salt}]$ where $[\text{surfactant}] = 0$, the salt concentration required for each series was calculated from the appropriate starting surfactant concentration, using a value of $\alpha = 0.3$ in eq 2, and assuming that α remains constant throughout the series. The value of 0.3 was obtained previously by EPR, but may also be determined from a PGSE-NMR experiment at the starting surfactant concentration.

Techniques

Small-Angle Neutron Scattering (SANS). The SANS measurements were performed as described previously^{3,9} on the fixed-geometry, time-of-flight LOQ diffractometer (ISIS Spallation Neutron Source, Oxfordshire, UK).

The intensity of the scattering data is given by $I(Q) = v_p\phi(\rho_1 - \rho_2)^2P(Q)S(Q) - B_{\text{inc}}$, where v_p is the volume of a particle (or in this case micelle), ϕ the volume fraction, and $(\rho_1 - \rho_2)^2$ the contrast term that describes the difference in scattering length density between the solvent (subscript 2) and the micelle (subscript 1). B_{inc} is the incoherent background scattering, while

$P(Q)$ and $S(Q)$ are respectively the form factor (which describes the particle morphology) and structure factor (which describes interparticle interactions). The scale factor $(v_p\phi(\rho_1 - \rho_2)^2)$ is calculated from the known sample composition and compared to the fitted value to check the suitability of the model.

The data were fitted using the FISH analysis program developed by Heenan.⁸ In this case the data were best described by a model for a ellipsoid interacting by an $S(Q)$ for charged spheres. The form factor is described elsewhere.⁹ (Polydisperse spheres were not appropriate.) Previously work in our group developed a more complex core-shell model to fit similar surfactant micelle data,⁹ using the degree of hydration of the headgroup region of the micelle measured by EPR and TRFQ derived aggregation numbers to constrain the SANS fit. For the micellar systems studied here, however, a simpler solid ellipse approach is entirely sufficient. There are two reasons for this: first, and in contrast to the previous SDS case, the scattering length density of the TMA⁺ headgroups ($\rho_{\text{slid}} = 0.36 \times 10^{10} \text{ cm}^{-2}$) is closely matched to that of the hydrocarbon tail ($\rho_{\text{slid}} = -0.36 \times 10^{10} \text{ cm}^{-2}$) value, and hence the principal contrast step lies at the headgroup/D₂O interface ($\rho_{\text{slid}}(\text{D}_2\text{O}) = 6.33 \times 10^{10} \text{ cm}^{-2}$). It is therefore extremely difficult to attempt to extract more detailed information without a high number of constraints in the model. Second, we are looking for significant changes in micelle shape only (or the absence thereof) and hence a more detailed picture of localized micelle structure is not required. This less complex approach was used successfully for DTAB and DTAC to illustrate the consistency in micelle morphology across the constant C_{aq} series.⁹

The structure factor $S(Q)$ was calculated using the Hayter and Penfold model¹⁰ for spheres of a given micellar concentration, charge, and ionic strength, incorporating refinements for low -volume fractions and a penetrating ionic background. This spherical approximation remains valid for ellipsoids of low axial ratio, as is the case here. The charge and screening length were the only parameters in the structure factor refined by the fit. Although in theory it is possible to extract the micellar charge (and therefore the degree of counterion dissociation via the aggregation number) from the fitted values for the structure factor, the fitting process can be insensitive to α . By comparison, the NMR approach is a more direct and sensitive probe of α , so we use the NMR data to find α and treat the $S(Q)$ from SANS empirically.

Pulsed-Field Gradient Spin-Echo NMR (PGSE-NMR). Measurements were conducted on a Bruker AMX360 NMR spectrometer using a stimulated echo sequence as described elsewhere.¹¹ This configuration uses a 5 mm diffusion probe (Cryomagnet Systems, Indianapolis) and a Bruker gradient spectroscopy accessory unit.

The self-diffusion coefficient D_s is extracted by fitting the integrals for a given peak to eq 4

$$A(\delta, G, \Delta) = A_0 \exp[-(kD_s)] \quad (4)$$

where A is the signal intensity and $k = -\gamma^2 G^2 \{ [30\Delta(\delta + \sigma)^2 - (10\delta^3 + 30\sigma\delta^2 + 35\sigma^2\delta + 14\sigma^3)]/30 \}$, where γ is the magnetogyric ratio, Δ the diffusion time, σ the gradient ramp time, δ the gradient pulse length, and G the gradient field strength.

Electrophoretic NMR (eNMR). Measurements were conducted on a Bruker AMX300 NMR spectrometer using a custom-designed glass U-tube of 2 mm outside diameter and coated internally with polyacrylamide to reduce electroosmosis.¹² The arrangement is held in the center of the active volume of a 10 mm diffusion probe (Cryomagnet Systems, Indianapolis,

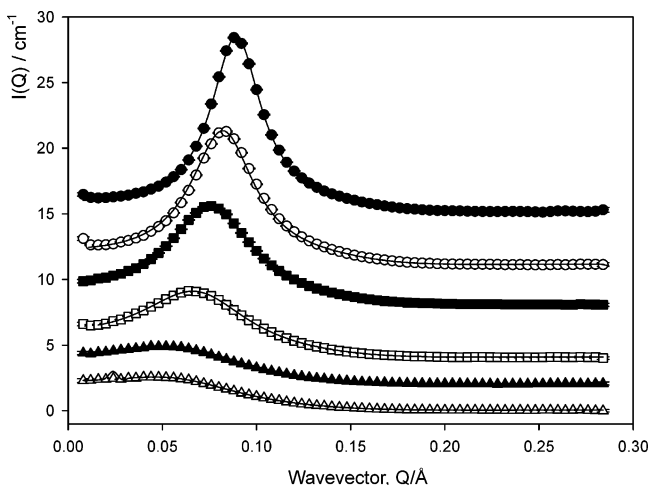


Figure 1. SANS data and fits from the TMADS/TMADCl constant C_{aq} series. $[TMA^+] = 16$ mM. Lines are fits to the ellipse model as described in the text. TMADS (mM)/TMADCl (mM): 400/0 (closed circles), 328/31 (open circles), 256/62 (closed squares), 184/92 (open squares), 112/123 (closed triangles), 6/154 (open triangles). For presentation purposes data and fits are scaled in intensity by a factor of 15, 11, 8, 6, 3, and 0, respectively.

IN). A constant current pulsed electric field generator designed by S. Woodward (University of North Carolina, Chapel Hill, NC) was used to deliver the current to two platinum wires extending just below the liquid surfaces.

In the presence of an electric field, charged micelles attain a drift velocity v that is superimposed upon their random diffusional motion. The displacement induced by the electric field, typically $20 \mu\text{m}$, was quantified using the spatial resolution of a simple form of NMR imaging.^{13,14} This coherent motion induced by the electric field results in a phase shift of the spin-echo given by

$$I(G, \delta, \Delta, v) = I_0 \cos(\gamma G \delta v \Delta) \exp\left[-\gamma^2 \delta^2 G^2 \left(\Delta - \frac{\delta}{3}\right) D_s\right] \quad (5)$$

where I is the integral of the relaxation-weighted Fourier transformed peak intensity in the absence (I_0) and presence ($I(G, \delta, \Delta, v)$) of flow and field gradients. The exponential term accounts for the attenuation due to diffusion. To maximize the electric field induced displacements with manageable pulsed electric fields, a diffusion time (Δ) of 0.5 s was used, which necessitated a stimulated echo sequence with $\tau = 10$ ms. The attenuation of the signal due to relaxation was therefore kept to a minimum, and was approximately 30%. Typically, gradient pulses were 1 ms in duration (δ) with intensity (G) 0.44 T/m. The sample concentrations for eNMR are limited by the sample conductivity, hence a lower concentration was used than for the SANS study.

Results and Discussion

We first discuss characterization of the micelle morphology by SANS and the prediction of eq 3 based on TRFQ, to provide a basis from which to interpret the NMR data. For experimental reasons, the SANS and NMR series were carried out at slightly different concentrations, but this has no significant impact on the conclusions.

SANS. Figure 1 shows the SANS data and fits to the ellipsoid model for a TMADS constant C_{aq} series. The corresponding parameters extracted from the fit are shown in Table 1. It is clear that micelle size and shape are invariant across the whole surfactant concentration range studied, consistent with behavior

for other constant C_{aq} series studied previously. In contrast to the approach used previously, for the data presented here no attempt was made to constrain the fit (for example, by limiting the ellipticity, aggregation number, or core radius) in a manner necessary for a more complex analysis of the data, rather the core radius was allowed to float freely. As the model is relatively insensitive to changes in ellipticity this was varied systematically to obtain the best fit to the data based on a nonlinear least-squares analysis.⁸ Generally X was increased if R became too large for the all-trans length of the surfactant. The quality of the fit was tested by comparison of the fitted and calculated scale factors as described previously. SANS aggregation numbers were obtained using a micellar volume calculated from the fit parameters: $V_{mic} = (4\pi R^3 X)/3$, where X is the ellipticity, and a calculated volume of the monomeric surfactant obtained from the sum of the contributing fragments ($V_{C12 \text{ chain}} = 358 \text{ \AA}^3$ (ref 15) + $V_{sulfate \text{ anion}} = 60.3 \text{ \AA}^3$ (ref 16) + $V_{TMA^+ \text{ ion}} = 155 \text{ \AA}^3$ —the latter was calculated from the relative molecular mass using an assumed mass density of 0.8 g cm^{-3}). $V_{monomer}$ was hence obtained as 573 or 526 \AA^3 allowing for a nominal 30% dissociation of the TMA^+ counterions. Aggregation numbers from SANS and those calculated from TRFQ measurements are given in Table 1. Good agreement between the two methods was observed; the SANS data are within the error on $V_{monomer}$. As a further check N may also be calculated from the volume of the micelle core. This was calculated using the overall fitted ellipticity ($X = 1.7$), using an assumed minor radius equal to the extended length of a C12 chain ($R = 16.7 \text{ \AA}$). Division by the volume of a C12 chain gives $N = 92$, in excellent agreement with TRFQ.

The SANS results are consistent with those of Berr et al.,¹⁷ who obtained an ellipticity of 1.4 with $N = 71$. Most importantly, it has been clearly shown that there is no significant change in micelle size or shape across the constant C_{aq} series.

PGSE NMR. As the counterion and surfactant have different chemical shifts, it is possible to study their individual mobilities. The micelle self-diffusion coefficient can be obtained from the dodecyl chain peak, which is an average mobility containing contributions from both monomeric and micellized surfactant. The monomer-corrected self-diffusion coefficient $D_{s(\text{micelle})}$ was obtained from eq 6, where x is a mole fraction. The monomer concentration is taken as the cmc = 5.5 mM for TMADS.⁴ Mobility of the (monomeric) dodecyl anion $D_{s(\text{monomer})}$ was obtained previously from a sodium dodecyl sulfate (SDS) sample below the cmc.

$$D_{s(\text{micelle})} = \frac{\langle D_{s(\text{measured})} \rangle - (x_{(\text{monomer})} \cdot D_{s(\text{monomer})})}{1 - x_{(\text{monomer})}} \quad (6)$$

1D spectra (not shown) demonstrated that there is no difference in the chemical shift of the tetramethylammonium (TMA^+) peak between the surfactant and the salt samples. The measured self-diffusion coefficient obtained from the TMA^+ peak therefore contains contributions from both bound and free counterions according to eq 7:

$$\langle D_{s(TMA^+)} \rangle = x_{(TMA^+)} \cdot D_{s(TMADCl)} + (1 - x_{(TMA^+)}) \cdot D_{s(\text{micelle})} \quad (7)$$

where $x_{(TMA^+)}$ is the mole fraction of TMA^+ counterions in solution, including contributions from monomeric surfactant,

TABLE 1: Parameters from Fits to SANS Data for the TMADS/TMADCl Constant C_{aq} Series ($[TMA^+] = 163$ mM)

[TMADS]/ mM	[TMADCl]/ mM	R / \AA (± 2 \AA)	ellipticity X	scale ratio (obs/calc)	$N(\text{SANS})$ (± 5)	$N(\text{TRFQ})^a$
400	0	19.8	1.7	0.9	83	92
328	31	19.7	1.7	0.9	82	92
256	62	20.0	1.7	1.0	86	92
184	92	19.8	1.7	1.0	83	92
112	123	19.8	1.7	1.3	83	92
6	154	16.7	1.65	0.8	83	92

^a Calculated based on eq 3, using values $N^0 = 61$ and $\gamma = 0.118$ derived from TRFQ.

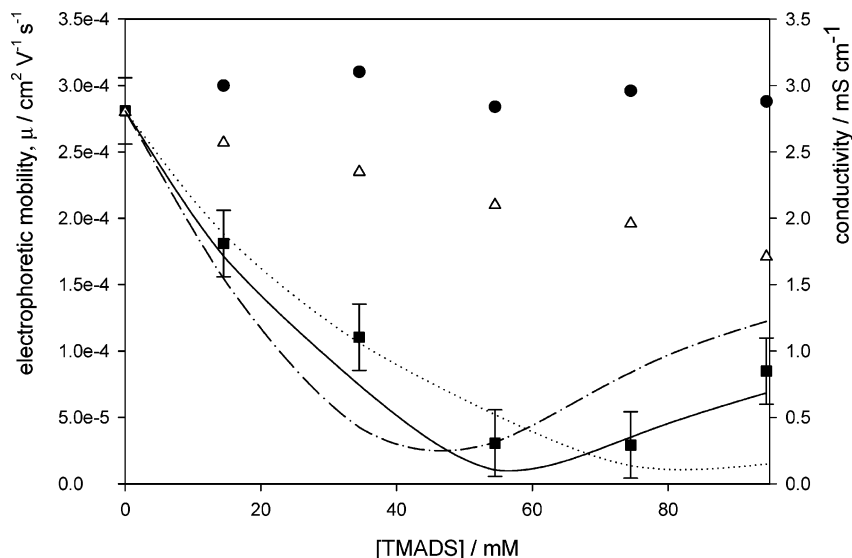


Figure 2. eNMR and conductivity data for the TMADS constant C_{aq} series $[TMA^+] = 39.9$ mM. Cosine fit to equation TMA^+ ions (filled squares) and micelles (filled circles). Also shown are conductivity data (open triangles). Lines are data from eq 10 for assumed values of α : 0.25 (dash-dot), 0.35 (solid), and 0.45 (dotted).

TABLE 2: Results from PGSE-NMR Experiments for the TMADS/TMADCl Constant C_{aq} series ($[TMA^+] = 39.9$ mM)

[TMADS]/ mM	[TMADCl]/ mM	$D_s(TMA^+)/$ $\times 10^{-6} \text{m}^2 \text{s}^{-1}$	$D_s(DS^-)/$ $\times 10^{-6} \text{m}^2 \text{s}^{-1}$	calcd α_{TMA^+}
100	0.0	9.2	1.1	0.35
80	7.2	10.9	1.6	0.39
60	14.5	12.3	1.8	0.35
40	21.8	14.6	2.3	0.33
20	29.0	18.0	3.3	0.29
0	36.3	22.0		

added salt, and those dissociated from the micelles:

$$X_{TMA^+} = \frac{[TMADCl] + [\text{monomer}] + \alpha([\text{surfactant}] - [\text{monomer}])}{[\text{surfactant}] + [TMADCl]} \quad (8)$$

where α is the degree of counterion dissociation. The self-diffusion coefficient of free TMA^+ ions was obtained by measuring a salt (TMADCl) solution.

Table 2 reports the self-diffusion coefficients for the micelle and counterion from a 100 mM TMADS constant C_{aq} series, including values for the monomeric dodecyl anion and free TMA^+ from a TMADCl solution. With increasing TMADS concentration the effective diffusion coefficient of the DS^- peak falls off slightly, reflecting the decreasing relative contribution from the monomer. The TMA^+ peak, meanwhile, has a more pronounced decrease, due simply to the greater difference in size between TMA^+ and the micelle.

From these values is it possible to calculate the degree of counterion dissociation using eqs 7 and 8. α_{TMA^+} is obtained as

0.33 ± 0.05 throughout the series, as shown in Table 2. This value of α_{TMA^+} is higher than the degree of counterion dissociation for TMADS obtained from conductivity measurements, from which $\alpha_{TMA^+} = \alpha_0 = 0.2$.⁴ However, $X_{(TMA^+)} = 0.33$ is in agreement with the value obtained from EPR measurements.⁵

eNMR. A similar set of equations may be written to obtain α_{TMA^+} from the electrophoretic mobility:

$$\mu_{\pm(DS^- \text{micelle})} = \frac{\mu_{\pm(DS^- \text{measured})} - (X_{(\text{monomer})} \cdot \mu_{\pm(DS^- \text{monomeric})})}{1 - X_{(\text{monomer})}} \quad (9)$$

$$\mu_{\pm(TMA^+)} = X_{(TMA^+)} \cdot \mu_{\pm(TMADCl)} + (1 - X_{(TMA^+)}) \cdot \mu_{\pm(DS^- \text{micelle})} \quad (10)$$

In this case, however the situation is slightly more complex; the application of an external field means that TMA^+ counterions bound to the negatively charged micelle are dragged in the opposite direction to free TMA^+ ions (dissociated surfactant counterions and TMA^+ salt cations). Hence, at a given stoichiometry, dependent on the degree of counterion binding, the overall mobility will pass through zero. As the eNMR experiment returns only the magnitude of the mobility, not the sign, a minimum in μ_{\pm} will be observed.

For 100 and 200 mM TMADS solutions the degree of counterion dissociation (in the absence of added salt) was calculated from the appropriate forms of eqs 9 and 10 to give $\alpha_{TMA^+} = 0.32$, in excellent agreement with the PGSE-NMR results.

Figure 2 shows the electrophoretic mobilities (corrected for the monomer contributions via the appropriate form of eq 7)

TABLE 3: eNMR Results for the TMADS/TMADCl Constant C_{aq} Series

[TMADS]/ mM	[TMADCl]/ mM	$\mu_{\pm}(\text{TMA}^+) \times 10^8/m^2 \text{ V}^{-1} \text{ s}^{-1}$	$\mu_{\pm}(\text{DS}^-) \times 10^8/m^2 \text{ V}^{-1} \text{ s}^{-1}$	ζ - potential/ mV	relative $\alpha(\text{TMA}^+)^a$	relative $\alpha(\text{TMA}^+)^b$
100	0	0.85	4.87	-58	0.33	0.32
80	7.2	2.93	5.00	-63	0.32	0.31
60	14.5	3.06	4.80	-57	0.34	0.32
40	21.8	1.10	5.24	-60	0.31	0.30
20	29.0	1.81	5.07	-59	0.34	0.32
0	36.3	2.81				

^a $N = 83$ (SANS at 400 mM). ^b $N = 80$ calculated for $[\text{TMA}^+] = C_{aq} = 39.9$ mM, using eq 2.

plotted against the monomer corrected surfactant concentration for a 100 mM constant C_{aq} series. Clearly, the micelle mobility remains unchanged across the series. Since we know from SANS that there is a constant aggregation number, this indicates a constant charge on the micelles and hence a constant degree of counterion dissociation, independent of surfactant and salt concentration. This is as expected within the constant C_{aq} framework. The electrophoretic mobility for any given surfactant concentration within the C_{aq} series can be predicted with reasonable accuracy from an appropriate form of eq 9, as shown by the solid line in Figure 2. Figure 2 confirms that $\alpha_{\text{TMA}^+} = 0.35$, as found from the diffusion experiments. This approach makes no assumptions regarding the size and shape of the micelles, save that N remains constant, as shown by SANS.

The conductivity (also plotted in Figure 2) shows a linear decrease with increasing surfactant concentration. Conductivity, being a macroscopic property, is determined by the concentration of the ions and their ionic mobility. The observed decrease in conductivity is therefore consistent with an increased proportion of the charge being associated with slower moving micelles. This tangentially highlights the usefulness of eNMR in terms of obtaining ion specific information that cannot be extracted from simple conductivity measurements.

The ζ potential at the micelle surface can be calculated from the electrophoretic mobilities using the large particle limit described by the Helmholtz–Schmoluchowski equation. As described previously¹⁸ the relative counterion dissociation may be calculated with reference to the known³ values of $\alpha(\text{Na}^+) = 0.27$, $N = 72$, and μ_{\pm} for SDS micelles in a 50 mM aqueous solution. Table 3 demonstrates the consistency across the constant C_{aq} series of $\alpha(\text{TMA}^+)$ found from this approach, which in contrast to the previous analysis is reliant on the absolute values of μ_{\pm} and N . For TMADS, N at 100 mM concentration was calculated from earlier TRFQ data via eq 3 where $N^0 = 61$, $\gamma = 0.118$, and $\alpha = 0.3$. The values of $\alpha(\text{TMA}^+)$ are on the order of 0.33–0.35, in excellent agreement with both PGSE-NMR, EPR, and other eNMR data. Comparing both constant C_{aq} series, results show that at these relatively high surfactant concentrations, and in the absence of added salt, that α_{TMA^+} remains approximately constant at 0.35, consistent with small changes in N in this concentration domain. The present work supports the aggregation number based determination of α according to eqs 1 and 2. This implies that either the conductiv-

ity method of determining α is not valid for TAADS or that α increases as a function of N . The experimental approach validated here will clearly be of use in addressing this possibility and has also established an ideal protocol for investigating the more complex behavior of TBADS.^{5,6}

Conclusions

Small-angle neutron scattering experiments have shown that the size and shape of TMADS micelles remain constant over a wide range of surfactant concentrations where TMADCl is added to keep the solution counterion concentration constant, i.e., TMADS conforms to the expected constant C_{aq} behavior. From PGSE-NMR and eNMR experiments the degree of counterion dissociation was shown to be 0.33. This value conflicts with the α_{TMA^+} obtained at the cmc from conductivity, but is in agreement with EPR studies which also obtain a higher value for α_{TMA^+} .

Acknowledgment. The Leverhulme trust and EPSRC (GR/S25456/01) (A.P. and P.C.G.), Swedish Research Council (VR) (P.S. and E.P.), and NIH (BB MBRS S06 GM48680-09) are thanked for funding.

References and Notes

- Bales, B. L. *J. Phys. Chem. B* **2001**, *105*, 6798.
- Quina, F. H.; Nassar, P. M.; Bonilha, J. B. S.; Bales, B. L. *J. Phys. Chem.* **1995**, *99*, 17028.
- Griffiths, P. C.; Paul, A.; Heenan, R. K.; Penfold, P.; Ranganathan, R.; Bales, B. L. *J. Phys. Chem. B* **2004**, *108* (12), 3810.
- Benraou, M.; Bales, B. L.; Zana, Z. *J. Phys. Chem. B* **2003**, *107*, 13432–13440.
- Bales, B. L.; Tiguida, K.; Zana, R. *J. Phys. Chem. B* **2003**, *108*, 13948–14955.
- Zana, R.; Benraou, M.; Bales, B. L. *J. Phys. Chem. B* **2004**, *108*, 18195–18203.
- Bales, B. L.; Zana, R. *Langmuir* **2004**, 1579–1581.
- Heenan, R. K. RAL Report 89-129, 1989.
- Griffiths, P. C.; Paul, A.; Penfold, J.; Heenan, R. K.; Bales, B. L. *J. Phys. Chem. B* **2004**, *108*, 3810–3838.
- Hayter, J. B.; Penfold, J. *Mol. Phys.* **1981**, *42*, 109.
- Davies, J. A.; Griffiths, P. C. *Macromolecules* **2003**, *36*, 950.
- Hjertén, S. *J. Chromatography* **1985**, *347*, 1991.
- Holz, M.; Müller, C. *Ber. Bunsen-Ges. Phys. Chem.* **1982**, *86*, 141.
- Holz, M. *Chem. Soc. Rev.* **1994**, *23*, 165.
- Tanford, C. J. *J. Phys. Chem.* **1974**, *78*, 2469.
- Hayter, J. B.; Penfold, J. *Colloid Polym. Sci.* **1983**, *261*, 1022.
- Berr, S. S.; et al. *J. Phys. Chem. B* **1986**, *90*, 6492.
- Griffiths, P. C.; Paul, A.; Stilbs, P.; Pettersson, E. P. *Langmuir* **2003**, *19*, 8605.